

## Friedelane Triterpenes from *Celastrus vulcanicola* as Photosynthetic Inhibitors

DAVID TORRES-ROMERO,<sup>†,‡</sup> BEATRIZ KING-DÍAZ,<sup>§</sup> RETO J. STRASSER,<sup>||</sup>  
 IGNACIO A. JIMÉNEZ,<sup>†</sup> BLAS LOTINA-HENNSEN,<sup>\*,§</sup> AND ISABEL L. BAZZOCCHI<sup>\*,†</sup>

<sup>†</sup>Instituto Universitario de Bio-Organica “Antonio González”, Universidad de La Laguna, Avenida Astrofísico Francisco Sánchez 2, 38206 La Laguna, Tenerife, Spain, <sup>‡</sup>Facultad de Química y Farmacia, Departamento de Bioquímica y Contaminación Ambiental, Universidad de El Salvador, Final 25 Av. Norte, San Salvador, El Salvador, <sup>§</sup>Departamento de Bioquímica, Facultad de Química, Universidad Nacional Autónoma de México, México D. F. 0451, Mexico, and <sup>||</sup>Bioenergetics Laboratory, University of Geneva, Chemin des Embouches 10, CH-1254 Jussy, Geneva, Switzerland

Five friedelane triterpenoids, epifriedelinol (**1**), friedelin (**2**), canophyllol (**3**), pulpononic acid (**4**) and 3-oxo-29-hydroxyfriedelane (**5**), were isolated from *Celastrus vulcanicola* (Celastraceae), and were identified by spectroscopic methods, comparison with authentic samples and reported data. In the search for potential herbicides, compounds **1–5** were evaluated for their photosynthetic inhibitory activity. Compound **1** acts as an energy transfer inhibitor, interacting and enhancing the light-activated Mg<sup>2+</sup>-ATPase, while **3** behaves as a Hill reaction inhibitor. The *in vivo* assays indicated that **1** and **3** act as selective postemergence herbicides at 100 μM by reducing biomass production in the weed *Physalis ixocarpa*. Moreover, results from Chl *a* fluorescence transients in leaves of *Lolium perenne* and *P. ixocarpa* suggest that both compounds affect photosynthesis efficiency of the chloroplasts as a response to a process of detoxification and repair. Thus, **1** and **3** reduce biomass by more complex mechanisms than only the damaging of the photosynthetic apparatus.

**KEYWORDS:** *Celastrus vulcanicola*; friedelane triterpenes; epifriedelinol; canophyllol; photophosphorylation-chlorophyll *a* fluorescence; herbicide

### INTRODUCTION

Triterpenes have attracted much interest due to their broad range of biological activities (*1, 2*), including phytotoxic (*3*) and photosynthesis inhibition activities (*4*). For example, lupane triterpenes isolated from *Melilotus messanensis* (Fabaceae) possess potential allelopathic activity in particular over dicotyledonous species (*3*), and 3,4-secofriedelan-3-oic acid isolated from *Maytenus imbricata* (Celastraceae) has been reported to inhibit several photosynthetic activities (*4*).

In a previous paper on bioactive constituents of *Celastrus vulcanicola* (Celastraceae), a subtropical woody vine distributed in Central America and the Caribbean, three new dihydro-β-agarofuran sesquiterpenes were isolated, and two of them behave as photosynthetic inhibitors (*5*). As a continuation of our research on *C. vulcanicola* we report herein the isolation of five friedelane triterpenoids, epifriedelinol (**1**) (*6*), friedelin (**2**) (*7*), canophyllol (**3**) (*7*), pulpononic acid (**4**) (*8*) and 3-oxo-29-hydroxyfriedelane (**5**) (*7*). In the search for natural photosynthetic inhibitors that could assist in the development of “green herbicides”, we investigated the mechanism of action on photosynthesis of triterpenes **1–5** and their targets on the electron transport chain and

H<sup>+</sup>-ATPase enzyme on thylakoids. Among the techniques suitable for assessing stress conditions in terms of photosynthesis, the measurement of direct fluorescence chlorophyll *a* (Chl *a*) in photosystem II (PSII) and the “JIP-test analysis” (i.e., the analysis of the O-J-I-P polyphasic rising transient) (*9*) combine several advantages: (i) simplicity and speed of the method, (ii) possibility of obtaining robust data sets, (iii) ease of repetition, (iv) straightforward processing of data and report findings, and (v) availability of instruments on the market and inexpensiveness of the measurement procedures.

### MATERIALS AND METHODS

**Plant Material.** *C. vulcanicola*, collected in June 2004 at the Montecristo National Park, province of Santa Ana, El Salvador, was identified by Jorge Monterrosa, and a voucher (J. Monterrosa & RCarballo 412) specimen was deposited in the Herbarium of Missouri Botanical Garden, USA.

**Isolation of Triterpenoids.** The dried stems (4.5 kg) of *C. vulcanicola* were sliced into chips, extracted with EtOH in a Soxhlet apparatus, and concentrated under reduced pressure. *n*-Hexane diethyl ether (10.1 g), dichloromethane (57.1 g), ethyl acetate (4.8 g) and aqueous (16.1 g) extracts were obtained from the EtOH extract (92.9 g). The bioactive CH<sub>2</sub>Cl<sub>2</sub> extract was further partitioned into CH<sub>2</sub>Cl<sub>2</sub>–H<sub>2</sub>O (1:1, v/v) solution. Removal of the CH<sub>2</sub>Cl<sub>2</sub> from the organic soluble fraction under reduced pressure yielded 57.1 g of residue, which was subjected to silica gel column chromatography and eluted with mixtures of *n*-hexane–EtOAc of increasing polarity to afford 4 fractions (I–IV). Fraction II was subjected

\*To whom correspondence should be addressed. For phytochemical studies (I.L.B.): tel, +34 922 318594; fax, +34 922 318571; e-mail, ilopez@ull.es. For photosynthetic studies (B.L.-H.): tel, +52 5622 5294; fax, +52 5622 5329; e-mail, blas@servidor.unam.mx.

to column chromatography over Sephadex LH-20, using a mixture of  $\text{CH}_2\text{Cl}_2$ -MeOH (1:1), and further purified by silica gel column chromatography and preparative TLC, developed with *n*-hexane-Et<sub>2</sub>O (10:2), to yield compounds **1** (0.7 g), **2** (1.2 g), **3** (2.3 g), **4** (0.6 g) and **5** (0.5 g). The compounds were identified using spectroscopic methods and gave values consistent with data reported in the literature (6–8).

**Chloroplast Isolation and Chlorophyll Determination.** Intact chloroplasts were obtained from spinach leaves (*Spinacea oleraceae* L) purchased from the local market as previously described (10, 11). Chloroplasts were suspended in a small volume of the following solution: 400 mM sucrose, 5 mM  $\text{MgCl}_2$ , 10 mM KCl, and 30 mM of the buffer tricine-KOH (pH 8.0). They were stored as a concentrated suspension in the dark for 1 h at 4 °C. The chlorophyll (Chl) concentration was measured according to Strain et al. (12).

**ATP Synthesis and Electron Flow Determinations.** ATP synthesis was determined titrimetrically using a microelectrode (Orion model 8103; Ross, Beverly, MA) connected to a Corning potentiometer model 12 (Corning Medical, Acton, MA), with an expanded scale and a Gilson recorder (Kipp & Zonen, Bohemia, NY) as previously reported (10, 13). Intact chloroplasts (20  $\mu\text{g}$  of Chl/mL) were broken before each assay by osmotic rupture in 3 mL of the nonbuffered solution containing 100 mM sorbitol, 10 mM KCl, 5 mM  $\text{MgCl}_2$ , 0.5 mM KCN, and 1 mM tricine-KOH at pH 8.0 in the presence of 50  $\mu\text{M}$  methylviologen (MV) and 1 mM adenosine diphosphate (ADP) at pH 6.7, and the pH was adjusted to 8.0 with 50 mM KOH. Alkalinization rates were measured in the linear part during illumination. The reaction was calibrated by back-titration with saturated HCl, and the ATP formed [ $\mu\text{mol}$  of ATP (mg of Chl)<sup>-1</sup> h<sup>-1</sup>] was measured.

**Measurements of Noncyclic Electron Transport Rate.** Light-induced noncyclic electron transport activity from water to MV was performed using a Clark type electrode. Basal electron transport was

determined by illuminating chloroplasts (20  $\mu\text{g}$  of Chl/mL) during 1 min in 3 mL of medium containing 100 mM sorbitol, 10 mM KCl, 5 mM  $\text{MgCl}_2$ , 0.5 mM KCN, 50  $\mu\text{M}$  MV and 15 mM tricine-KOH (pH 8.0) as previously described (10, 14, 15). Phosphorylating noncyclic electron transport rate was measured as basal electron transport from water to MV except that 1 mM ADP and 3 mM  $\text{KH}_2\text{PO}_4$  were added. Uncoupled

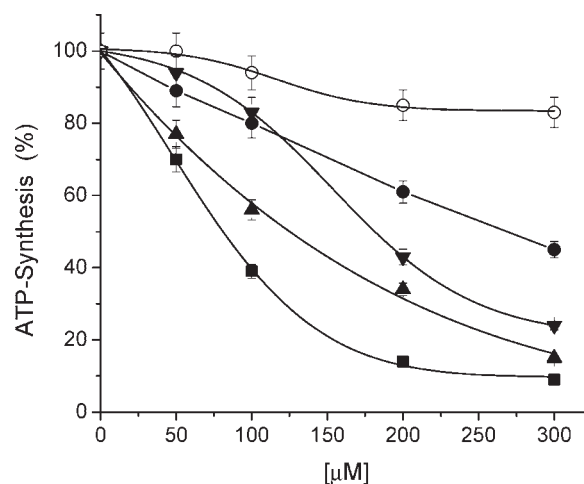


**Figure 3.** Inhibitory effect of friedelane triterpenoids: **1** (■), **2** (●), **3** (▲), **4** (▼) and **5** (○) on ATP synthesis. Control rate values were 746 (**1**) and 1551 (**2–5**)  $\mu\text{M}$  ATP · h<sup>-1</sup> · (mg of Chl)<sup>-1</sup>. Data are average of three replicates. Other conditions are as described in Materials and Methods.

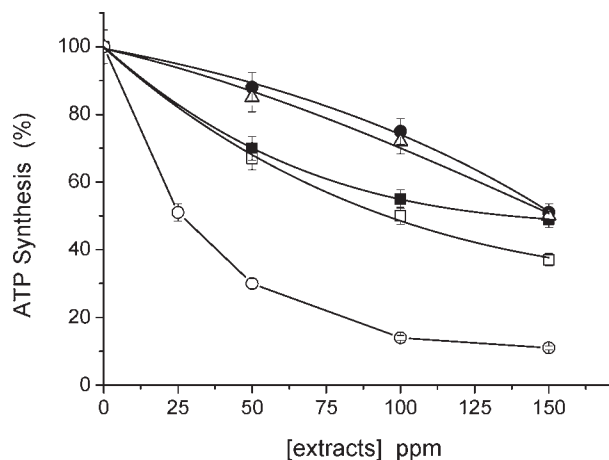


**Figure 1.** Effect of *Celastrus vulcanicola* extracts: aqueous (■), ethanol (●), dichloromethane (○), ethyl acetate (△) and *n*-hexane diethyl ether (□) on ATP synthesis. Control rate values were 494 (■, ●, △) and 546 (□, ○)  $\mu\text{M}$  ATP · h<sup>-1</sup> · (mg of Chl)<sup>-1</sup>. Data are average of three replicates. Other conditions as indicated in Materials and Methods.

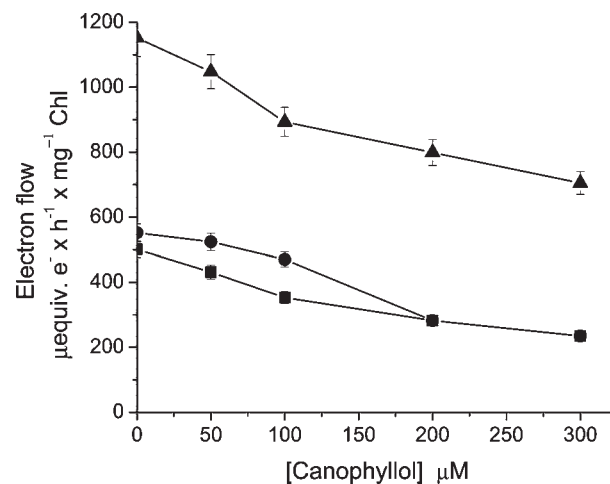


**Figure 4.** Effect of canophyllol (**3**) on electron flow from water to MV in spinach chloroplasts under basal (■), phosphorylating (●), and uncoupled (▲) conditions. Other conditions are as indicated in Materials and Methods. Data are averages of three replicates.

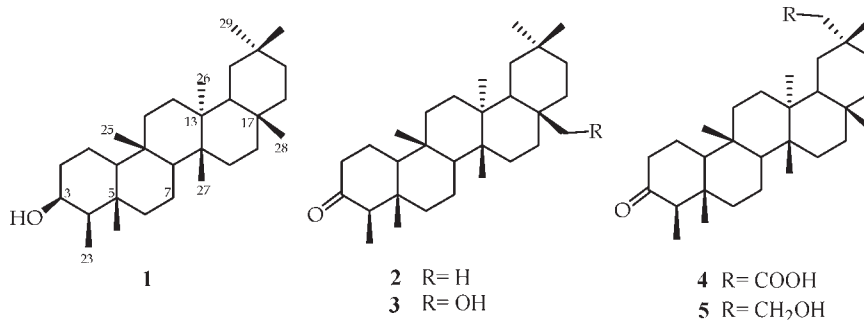


**Figure 2.** Structures of friedelane triterpenoids **1–5**.

**Table 1.** Effect of Compounds **1** and **3** and  $\text{NH}_4\text{Cl}$  on  $\text{Mg}^{2+}$ -ATPase Bound to Thylakoid Membranes<sup>a</sup>

compound	$\mu\text{M Pi mg}^{-1} \text{Chl h}^{-1}$	act. (%)
<b>1 (<math>\mu\text{M}</math>)</b>		
0	142 ± 7.1	100
100	156 ± 7.8	110
200	159 ± 8.0	112
300	175 ± 8.8	123
<b>3 (<math>\mu\text{M}</math>)</b>		
0	154 ± 7.7	100
100	169 ± 8.5	110
200	179 ± 9.0	116
300	194 ± 9.7	126
<b><math>\text{NH}_4\text{Cl}</math> (mM)</b>		
0	154 ± 7.7	100
1	197 ± 9.9	128
2	388 ± 19.4	252
3	357 ± 17.9	234

<sup>a</sup>Data are average of three replicates.**Table 2.** Effect of Canophyllol (**3**) on Uncoupled PSII Electron Transport and Partial Reactions<sup>a</sup>

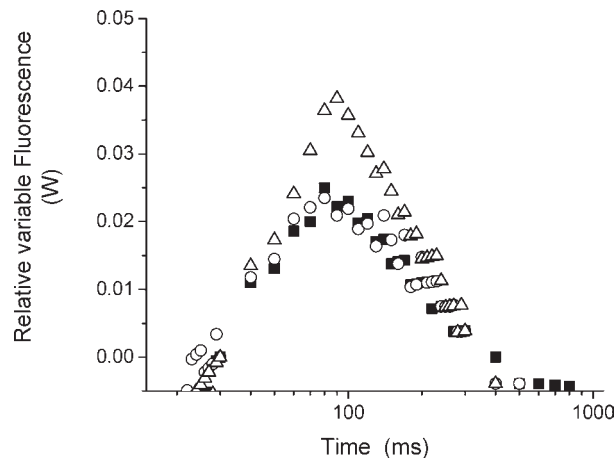
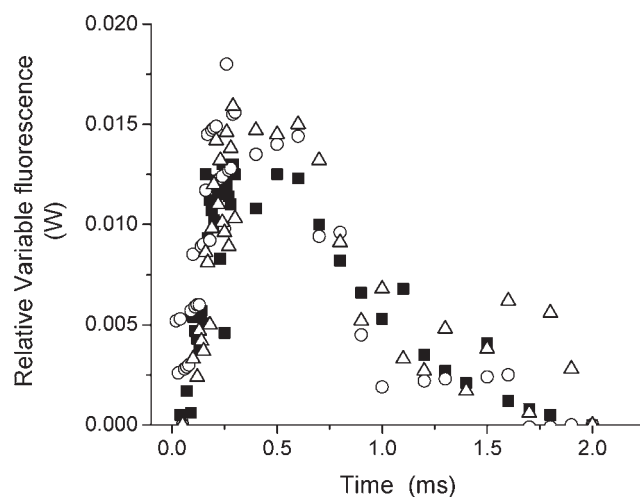
concn ( $\mu\text{M}$ )	$\text{H}_2\text{O}$ to DCBQ		$\text{H}_2\text{O}$ to SiMo		DCP to DCPIP	
	<i>b</i>	<i>c</i>	<i>b</i>	<i>c</i>	<i>b</i>	<i>c</i>
0	270 ± 13.5	100	200 ± 10.0	100	169 ± 8.5	100
50	240 ± 12.0	89	120 ± 6.0	60	177 ± 8.9	105
100	184 ± 9.2	68	40 ± 2.0	20	183 ± 9.2	108
200	135 ± 6.8	50	20 ± 1.0	100	161 ± 8.0	95
300	118 ± 5.9	44	0	0	169 ± 8.5	100

<sup>a</sup>Data are average of three replicates. <sup>b</sup>Photosystem and partial reactions rate values in  $\mu\text{equiv e}^-/\text{h mg Chl}$ . <sup>c</sup>100% is the activity of the control.

electron transport was tested in the medium for basal electron transport, and 6 mM  $\text{NH}_4\text{Cl}$  was added as uncoupler.

**Uncoupled Photosystem II (PSII) and Photosystem I (PSI) Electron Flow Determination.** Uncoupled electron transport rate from water to 2,5-dichloro-1,4-benzoquinone (DCBQ) (*16*) was measured in the medium for PSII reaction mixture containing 100 mM sorbitol, 10 mM KCl, 5 mM  $\text{MgCl}_2$ , 0.5 mM KCN and 15 mM tricine-KOH (pH 8.0), with the addition of 100  $\mu\text{M}$  DCBQ, 1  $\mu\text{M}$  2,5-dibromo-6-isopropyl-3-methyl-1,4-benzoquinone (DBMIB) and 6 mM  $\text{NH}_4\text{Cl}$  and chloroplasts (20  $\mu\text{g}$  of Chl/mL), the reaction mixture (3 mL) was illuminated during 1 min. Uncoupled partial reaction of PSII electron transport rate from water to sodium silicomolybdate (SiMo) was determined in the same way as for PSII, except that 100  $\mu\text{M}$  DCBQ and 1  $\mu\text{M}$  DBMIB were changed by 200  $\mu\text{M}$  SiMo and 10  $\mu\text{M}$  [3-(3,4-dichlorophenyl)-1,1-dimethylurea] DCMU (*17*). Uncoupled PSI electron transport rate was determined on chloroplasts (20  $\mu\text{g}$  Chl/mL) using 3 mL of the basal electron transport medium plus 10  $\mu\text{M}$  DCMU, 100  $\mu\text{M}$  2,6-dichlorophenol indophenol (DCPIP), 300  $\mu\text{M}$  sodium ascorbate and 6 mM  $\text{NH}_4\text{Cl}$  (*10*, *11*, *18*). These electron flow activities were monitored with a Yellow Springs Instrument (YSI) oxygen monitor, model 5300A, using a Clark type electrode. All reaction mixtures were illuminated with actinic light from a projector lamp (GAF 2660) and passed through a 5 cm filter of a 1%  $\text{CuSO}_4$  solution. The temperature was 20 °C, and for each reaction a blank experiment was performed with chloroplasts in the reaction medium. The  $I_{50}$  value (concentration producing 50% inhibition) for each activity was determined from plots of the activity at different concentrations of compound.

**$\text{Mg}^{2+}$ -ATPase Activity Assays.** Chloroplasts were isolated from 30 to 40 g of spinach leaves, which were ground in 160 mL of medium containing 350 mM sorbitol, 5 mM ascorbic acid and 20 mM 2-(*N*-morpholino)ethanesulfonic acid (MES) at pH 6.5. Chloroplasts were centrifuged at 3000g for 60 s, washed once in 40 mL of grinding medium,

**Figure 5.** The fluorescence transient curves normalized between  $F_{30\text{ms}}$  and  $F_P$ , expressed as  $W_{30\text{ms-P}} = (F_m - F_t)/(F_m - F_{30\text{ms}})$ , show the appearance of an I-band at 100 ms in thylakoids infiltrated with epifriedelinol (**1**) at 150 (■), 300 (○) and 450 (Δ)  $\mu\text{M}$ . Data are averages of five replicates.**Figure 6.** Appearance of a K-band at about 300  $\mu\text{s}$ . The ordinate is the difference between the  $W$  of the treated thylakoids with canophyllol (**3**) and the  $W$  of the control.  $W$  is the relative variable fluorescence between  $F_0$  and  $F_t$ , and calculated as  $W_t = F_{Vt}/(F_J - F_0) = (F_t - F_0)/(F_J - F_0)$ . Thylakoids were infiltrated with **3** at 150 (■), 300 (○) and 450 (Δ)  $\mu\text{M}$ . Data are averages of five replicates.

and resuspended in 35 mM HEPES buffer (pH 7.6). Light-triggered  $\text{Mg}^{2+}$ -ATPase activity associated to thylakoid membranes was measured as previously described (*11*), and released inorganic P was measured as reported (*19*).

**Chlorophyll *a* Fluorescence Measurements.** Chlorophyll *a* fluorescence was measured at room temperature with a Hansatech Fluorescence Handy PEA (plant efficiency analyzer) in 5 min dark-adapted chloroplasts (20  $\mu\text{g}/\text{mL}$ ) (*10*, *14*, *20*), using red light intensity (broad band 650 nm) of 3000  $\mu\text{mol m}^{-2} \text{s}^{-1}$ , provided by an array of three light emitting diodes. The pulse duration was 2 s. The reaction medium was that employed in basal noncyclic electron transport measurements without MV. To monitor Chl *a* fluorescence transients, aliquots of dark adapted thylakoids containing 20  $\mu\text{g}$  of Chl were placed by gravity on filter paper with a dot-blot apparatus (Bio-Rad, United States). In order to ensure a homogeneous and reproducible distribution of thylakoids on the filter paper, they were dipped immediately in 3 mL of basal electron transport medium with different concentrations of the tested compound. Different photosynthetic parameters associated with PSII were obtained according to the equations of the O-J-I-P test, using the Bioanalyser program (*14*, *20*, *21*).  $F_0$ , fluorescence intensity level at 20  $\mu\text{s}$  when plastoquinone electron acceptor

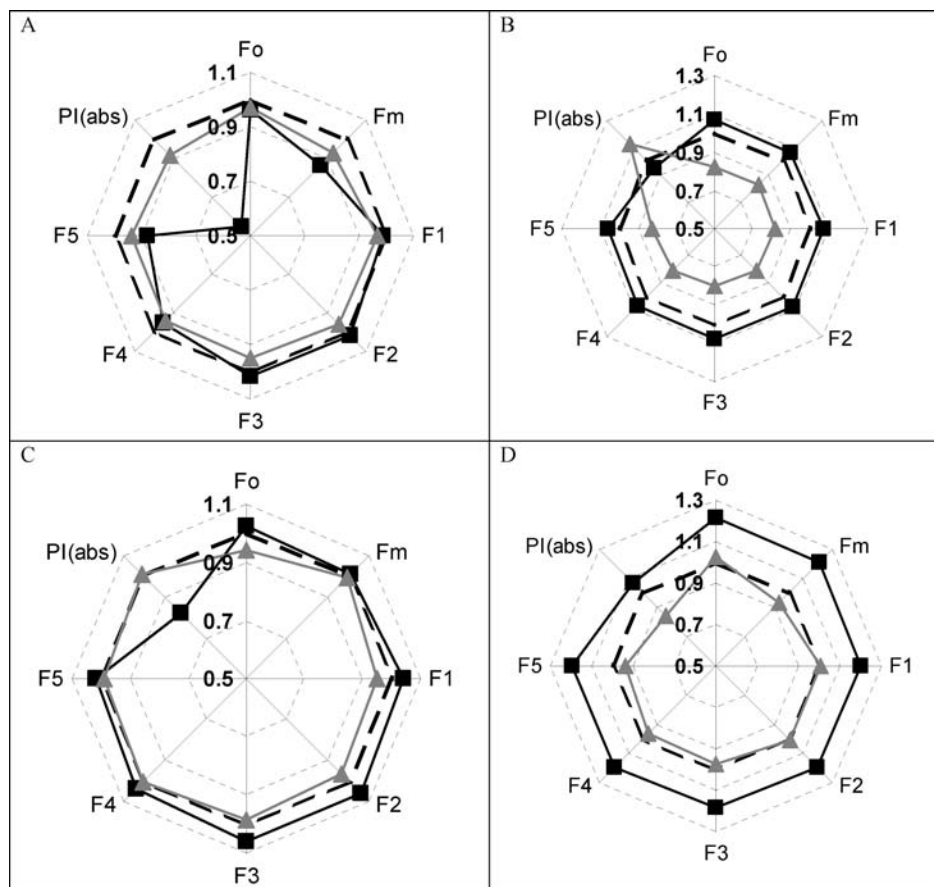


**Figure 7.** Radar plot graphs show the effects of **3** at 24 (A), 48 (B) and 72 h (C) and **1** at 72 h (D) on chlorophyll *a* fluorescence transients of *L. perenne* leaves from plants grown in a greenhouse. Both compounds were infiltrated at 100  $\mu\text{M}$  (black ■, black line) and 200  $\mu\text{M}$  (gray triangle, gray line). The effects of compounds **1** and **3** were compared to the control plant (dashed black line).

pool ( $Q_A$ ) is fully oxidized;  $F_m$ , fluorescence level when  $Q_A$  is transiently fully reduced;  $F_v$ , variable component of fluorescence obtained by subtraction of  $F_0$  from the  $F_m$  value;  $F_1$ , fluorescence intensity level at 50  $\mu\text{s}$ ,  $F_2$  at 100  $\mu\text{s}$ ,  $F_3$  at 300  $\mu\text{s}$ ,  $F_4$  at 2 ms and  $F_5$  at 30 ms.  $\text{PI}_{(\text{abs})} = [\text{RC}/\text{ABS}][\phi_{\text{P}_0}/(1 - \phi_{\text{P}_0})][\psi_{\text{E}_0}/(1 - \psi_{\text{E}_0})]$ , performance index (PI) on absorption basis, where  $\phi_{\text{P}_0}$  is the maximum quantum yield of primary photochemistry at  $t = 0$ , and  $\psi_{\text{E}_0}$  is the probability (at time 0) that a trapped exciton can move an electron into the electron transport chain beyond  $Q_A^-$  (22).

**Plant Material for *in Vivo* Assays.** Seeds of *Physalis ixocarpa* and *Lolium perenne*, weed species, were sown in 12 cm diameter pots and were watered daily in the greenhouse at 25 to 30  $^{\circ}\text{C}$ . After 15 and 18 days of emergence for *P. ixocarpa* and *L. perenne*, respectively, plants were selected for similar size and were sprayed manually with compounds at concentrations of 100 and 200  $\mu\text{M}$  (20 mM of stock compounds was dissolved in DMSO). An aliquot of this solution was taken to obtain the desired concentration in an aqueous suspension containing 0.05% w/v of Tween-20 (polyoxyethylensorbitan monolaurate). The control group was sprayed with distilled water containing the same amount of DMSO and Tween-20.

**Chlorophyll *a* Fluorescence Determination in Intact Leaves *in Vivo*.** Chlorophyll *a* fluorescence was performed for control plants and plants sprayed with concentrations of 100 and 200  $\mu\text{M}$  of each tested compound. After being kept in the dark for 15 min, the leaves were excited by saturating light from an array of three light-emitting diodes delivering 3000  $\mu\text{mol}$  of photons  $\text{m}^{-2} \text{s}^{-1}$  of red light (peak at 650 nm). Chlorophyll *a* fluorescence induction curves were measured at room temperature with a portable Handy PEA (plant efficiency analyzer, Kings Lynn, U.K.) apparatus (23).

Radial plots have existed for years as important descriptive tools for multivariate data. In general, the common feature of radial plots is the fact that they are a circular graphing method. They have a series of spokes or

rays projecting from a central point, with each ray representing a different variable label (24). In this study, the Chl *a* fluorescence transients  $F_1$ ,  $F_2$ ,  $F_3$ ,  $F_4$ ,  $F_5$ ,  $F_m$  and the photosynthetic efficiency, expressed as  $\text{PI}_{(\text{abs})}$ , are represented in each ray. They appear as a radar plot with the lengths of the rays indicating each value. These values were typically normalized, the central point of the radar graph has the value 0.5 and the control corresponds to the unit.

**Dry Biomass Determination.** After 15 days of treatment with tested compounds, all plants were harvested at ground level and dried in an oven at 65  $^{\circ}\text{C}$  until constant weight. Then the dry mass was determined (23).

## RESULTS AND DISCUSSION

**Isolation of Friedelane Triterpenoids.** The stems of *Celastrus vulcanicola* were successively extracted with *n*-hexane diethyl ether, dichloromethane, ethyl acetate, and ethanol and aqueous. The obtained extracts were tested on ATP synthesis on isolated spinach chloroplasts as a screening method for further fractionation. All the extracts showed inhibitory effect on ATP synthesis (Figure 1), the dichloromethane being the most active one. Therefore, this was selected for further chromatographic studies to search for the bioactive metabolites. Five known friedelane triterpenoids were isolated from the dichloromethane extract. They were identified by spectroscopic methods, comparison with authentic samples and data reported in the literature as epifriedelinol (**1**), friedelin (**2**), canophyllol (**3**), pulpononic acid (**4**) and 3-oxo-29-hydroxyfriedelane (**5**) (6–8) (Figure 2).

**Effect of Friedelane Triterpenoids on Photophosphorylation.** Compounds **1–5** were monitored by the inhibition of photophosphorylation from water to MV in freshly lysed chloroplasts.



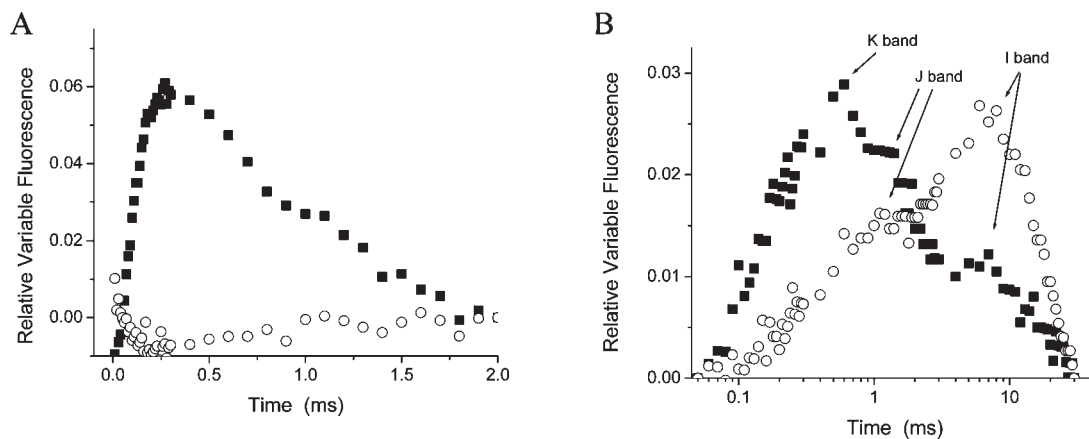


**Figure 8.** Appearance of a K-band in the leaves of *L. perenne* sprayed with 100  $\mu\text{M}$  **3** (■) at 24 h (A), and appearance of a J-band with 100  $\mu\text{M}$  (■) and 200  $\mu\text{M}$  (○) **3** at 72 h (B). Data are averages of five replicates.

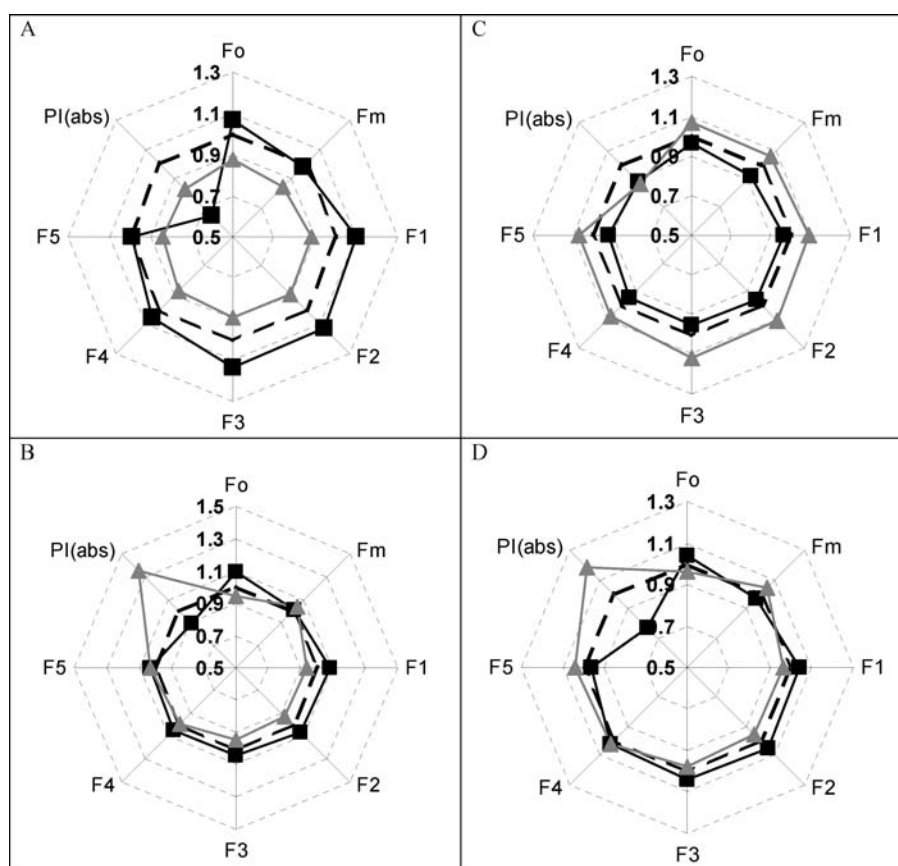


**Figure 9.** Radar plot graphs show the effects of **1** and **3** at 100  $\mu\text{M}$  (black ■, black line) and 200  $\mu\text{M}$  (gray ▲, gray line) on chlorophyll *a* fluorescence transients of *P. ixocarpa* leaves from plants grown in a greenhouse. Panels A and B correspond to 48 and 72 h of treatment with **1**, respectively. Panel C corresponds to 48 h and panel D to 72 h of treatment with **3**. The effects of both compounds were compared to the control plant (dashed black line).

Epifriedelinol (**1**) and canophyllol (**3**) were identified as the most bioactive compounds in a concentration dependent manner, with  $I_{50}$  values of 82 and 124  $\mu\text{M}$ , respectively. Moreover, the  $I_{50}$  values of **2** and **4** were 181.5 and 268.6  $\mu\text{M}$  (Figure 3), respectively, and **5** showed the lowest inhibiting effect on ATP formation, thus they were not studied further.

In order to investigate the potential of compounds **1** and **3** as natural herbicides, their photosynthetic inhibitory effects were studied. Thus, their effect on noncyclic electron transport from water to MV was evaluated under basal, phosphorylation, and uncoupled conditions. Compound **1** did not show inhibitory activity on the electron transport process at any of the three

tested states (data not shown). Moreover, compound **3** inhibited partially the electron transport to different degrees under all the assayed conditions as its concentration increased up to 300  $\mu\text{M}$  (Figure 4). Furthermore, when the light-activated  $\text{Mg}^{2+}$ -ATPase bound to thylakoid membranes was determined in the presence of increasing concentrations of **1** and **3** up to 300  $\mu\text{M}$ , and using ammonium chloride as positive control, both compounds enhanced moderately this activity (Table 1), indicating that they affect the  $\Delta\text{pH}$  and thus avoiding the ATP formation.

These results indicate that **1** has two targets of interaction: one is a decrease of the  $\Delta\text{pH}$  resulting in the ATP not being synthesized and the second by interacting and inhibiting the

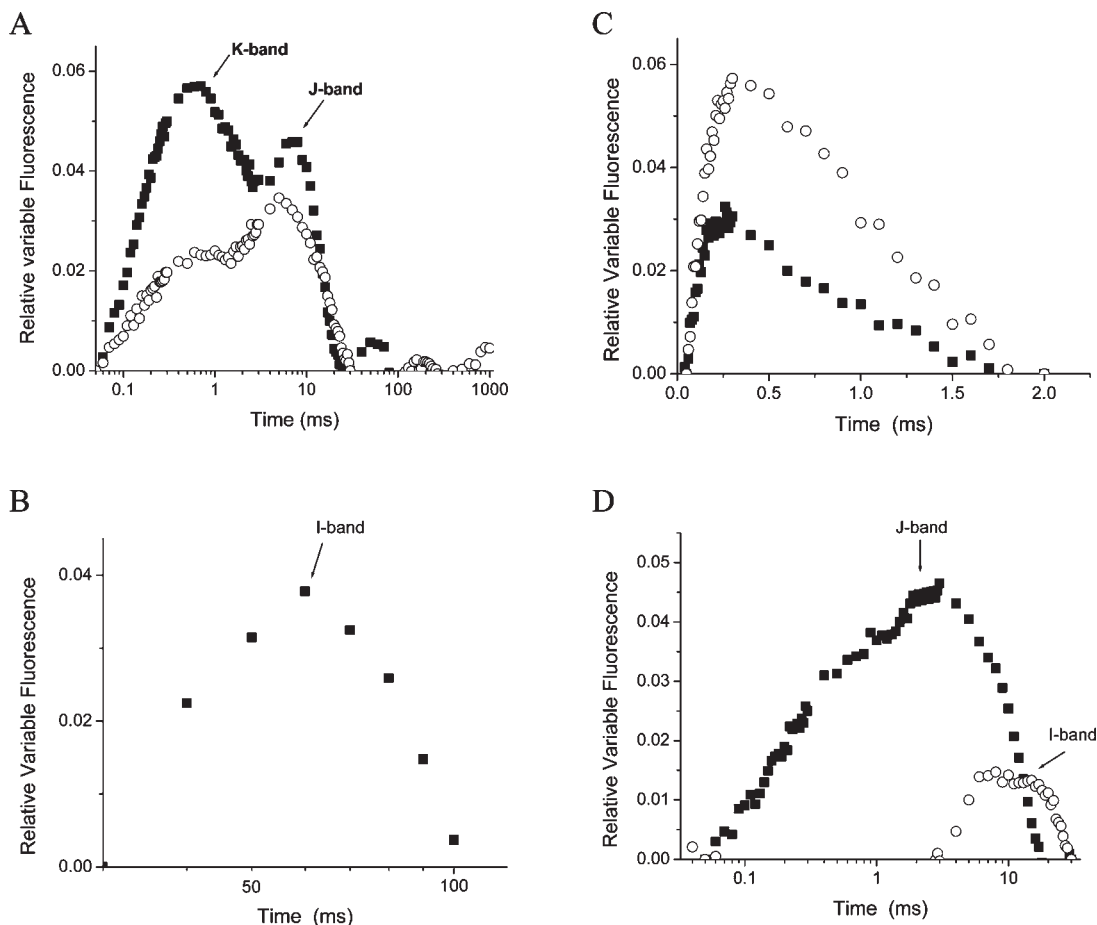


**Figure 10.** Appearance of bands from fluorescence of chlorophyll *a* transients of leaves of *P. ixocarpa* after 48 h sprayed with 100  $\mu\text{M}$  (■) and 200  $\mu\text{M}$  (○) of **1** (A and B) and **3** (C and D). In panels A and C, a K-band appears at about 300  $\mu\text{s}$  at 48 h after treatment, and panels B and D show the appearance of I- and J-bands after 72 h of treatment. Data are averages of five replicates.

$\text{Mg}^{2+}$ -ATPase in thylakoids. **3** acts as a Hill reaction inhibitor target on PSII electron flow from water to DCBQ (Table 2).

**Chlorophyll *a* Fluorescence Measurements.** Chl *a* fluorescence transients in the presence of compounds **1** or **3** were measured on isolated freshly lysed chloroplasts to corroborate their interaction sites on photosynthesis. The transient curves obtained for **1** were normalized between  $F_{30\text{ms}}$  and  $F_p$ , expressed as  $W_{30\text{ms-P}} = (F_m - F_t)/(F_m - F_{30\text{ms}})$  and plotted. These curves showed the appearance of an I-band close to 100 ms (Figure 5). This band is indicative of the increasing IP phase from  $F_{80\text{ms}}$  to  $F_m$ , its amplitude is a measure of the amount of reduced acceptors end at the PSI of thylakoids, and it represents the last and rate-limiting step of the photosynthetic electron transport chain (25). Therefore, **1** has two targets of interaction—inhibition, one at the reducing side of PSI and the other at the  $\text{Mg}^{2+}$ -ATPase complex. Since **3** inhibits PSII, its effect on Chl *a* fluorescence transients was measured. The transients of the relative variable fluorescence were normalized between  $F_j$  and  $F_0$ , and expressed as  $W_t = F_{vt}/(F_j - F_0) = (F_t - F_0)/(F_j - F_0)$ . The results show a fast rise at about 300  $\mu\text{s}$  (K-band) (Figure 6). Therefore, **3** has two targets: one is at the oxygen-evolving complex (OEC) of the PSII by inhibiting the water splitting enzyme and the second by interacting and enhancing the light-activated  $\text{Mg}^{2+}$ -ATPase (Table 1). The water splitting enzyme is also inhibited by other natural products as pachypodol (26), labdane-8 $\alpha$ ,15-diol (27) and 1-*O*-acetyl-12,13-dihydroanthorrhizol (28).

**In Vivo Assays.** To investigate if compounds **1** and **3** behave as potential herbicides, their effects on intact leaves of *L. perenne* and *P. ixocarpa* were determined. Thus, the Chl *a* fluorescence

transients and the photosynthetic efficiency, expressed as PI(abs), were measured at 24, 48, and 72 h in control and treated plants.

The Chl *a* fluorescence transients in *L. perenne* plants treated with 100  $\mu\text{M}$  **3**, compared with the control transients, show that the PI(abs) decreases by around 50% at 24 h (Figure 7A), while at 48 h this parameter was almost unaffected (Figure 7B), and at 72 h of treatment the PI(abs) only decreases by 15% (Figure 7C). However, *L. perenne* plants treated with 200  $\mu\text{M}$  **3** show an insignificant effect on PI(abs) at 24, 48, and 72 h (Figure 7A–C). Therefore, the quenching effect of **3** at 100  $\mu\text{M}$  observed on the transients  $F_m$ , F4 and F5 at 24 h is a sign of damage of the photosynthetic apparatus in *L. perenne*, and it is related to the K-band appearance (Figure 8A), indicating that the donor side of PSII is damaged. However, at 48 h the K-band disappeared (data not shown), and at 72 h after treatment with 100  $\mu\text{M}$  **3**, the K-band reappears, this behavior indicates that the plant has the capacity to repair its photosynthetic apparatus in an attempt to resist the biotic or abiotic stress. Moreover, **3** at 200  $\mu\text{M}$  induces the formation of a J-band (transients of the relative variable fluorescence normalized between  $F_{30\text{ms}}$  and  $F_0$  and expressed as  $W_t = F_{vt}/(F_{30\text{ms}} - F_0) = (F_t - F_0)/(F_{30\text{ms}} - F_0)$  show a fast rise at about 2 ms) (Figure 8B). This indicates that **3** affects the acceptor side of PSII in a similar way to the known herbicide diuron. Furthermore, an I band appears with **3** at 200  $\mu\text{M}$  (Figure 8B). Therefore, the action mechanism of canophyllol (**3**) at 100  $\mu\text{M}$  changes over time in contact with the *L. perenne* leaves (Figure 8A, B). We propose that **3** is metabolized by the plant and at 72 h a new compound with different structure induces the appearance of the J- and I-bands.

**Table 3.** Effect<sup>a</sup> of Epifriedelinol (**1**) and Canophyllol (**3**) on Biomass Production Estimated by Measuring the Dry Weight of *Physalis ixocarpa* and *Lolium perenne* Plants Growth<sup>b</sup>

concn ( $\mu\text{M}$ )	<i>P. ixocarpa</i>		<i>L. perenne</i>	
	(g)	(%)	(g)	(%)
<b>1</b>				
0	0.255 $\pm$ 0.03 <sup>c</sup>	100	0.141 $\pm$ 0.03	100
100	0.060 $\pm$ 0.02	23.2	0.092 $\pm$ 0.03	79.6
200	0.258 $\pm$ 0.04	101.3	0.105 $\pm$ 0.02	91.2
<b>3</b>				
100	0.208 $\pm$ 0.02	81.5	0.135 $\pm$ 0.09	117.1
200	0.251 $\pm$ 0.00	99.0	0.162 $\pm$ 0.07	140.3

<sup>a</sup> After 14 days of application. <sup>b</sup> Data are averages of three replicates. <sup>c</sup> The  $\pm$ SE were calculated with the program Origin 6.0 Professional.

Leaves of *L. perenne* treated after 24 and 48 h with compound **1** have no effect on the OJIP transients (data not shown). Moreover, at 72 h of treatment with 100  $\mu\text{M}$  **1**, the transients and the PI(abs) increase by 20% and 10%, respectively (**Figure 7D**), while at 200  $\mu\text{M}$  the PI(abs) decreases by 12%, and the transients are almost unaffected.

In order to know if compounds **1** and **3** have selectivity as herbicides, their effects on *P. ixocarpa* plants after 24, 48, and 72 h of treatment were examined. The fluorescence transients of Chl *a* at 24 h after treatment with both compounds were not affected (data not shown). However, the *P. ixocarpa* leaves treated with 100  $\mu\text{M}$  **1** at 48 h show that PI(abs) decreases by 40% and the fluorescence of Chl *a* transients ( $F_0$ ,  $F_1$ ,  $F_2$ ,  $F_3$  and  $F_4$ ) increases by 10% (**Figure 9A**), while at 200  $\mu\text{M}$  these parameters decrease by 15% and 10%, respectively. For both concentrations K- and J-bands appear (**Figure 10A**), indicating that **1** affects the donor and the acceptor sides of PSII. Subsequently, the leaves at 72 h after treatment with 100  $\mu\text{M}$  **1** showed a slight recovery, which was indicated by the increase of the PI(abs) value compared with the control leaves (**Figure 9B**), and it should be noted that K- and J-bands disappear and an I-band starts to appear (**Figure 10B**). The behavior of **3** on *P. ixocarpa* at 100 and 200  $\mu\text{M}$  and 48 h of treatment decreased the PI(abs) by 10% (**Figure 9C**), and induced the appearance of the K-band (**Figure 10C**). Moreover, after 72 h of treatment with 100  $\mu\text{M}$  **3**, the PI(abs) decreased by 25% and the formation of a J-band was induced. However, the PI(abs) increased by 10% at 200  $\mu\text{M}$  **3**, and the K-band was lost and a small I-band was induced (**Figure 10D**). Therefore, these changes of PI(abs) at 48 and 72 h, and the loss of K-bands at 72 h suggest that *P. ixocarpa* plant can respond to the effect of friedelane triterpenoids with processes of detoxification and repair or by metabolizing the triterpenoids (29).

**Biomass Production.** This was estimated by measuring the dry weight of *P. ixocarpa* and *L. perenne* plants grown in the presence or absence of 100 and 200  $\mu\text{M}$  **1** and **3** (**Table 3**). After 14 days of application of **1** at 100  $\mu\text{M}$ , the total dry biomass decreased by 76.8% in *P. ixocarpa* plants, while the dry biomass was unaffected at 200  $\mu\text{M}$ . Furthermore, the dry weight of *L. perenne* plants decreased by 20.4% at 100  $\mu\text{M}$ , and by 8.8% at 200  $\mu\text{M}$ . Moreover, compound **3** only inhibited the growth of *P. ixocarpa* plants at 100  $\mu\text{M}$  (18.5%) and has no effect at 200  $\mu\text{M}$ . The biomass production of *L. perenne* was enhanced by 17% and 40% at 100 and 200  $\mu\text{M}$ , respectively (**Table 3**).

As epifriedelinol (**1**) and canophyllol (**3**) induce only minor damage to the photosynthetic apparatus at the electron transport level, other mechanisms are involved in biomass reduction of *P. ixocarpa* by these natural products.

## LITERATURE CITED

- (1) Dzubak, P.; Hajduch, M.; Vydra, D.; Hustova, A.; Kvasnica, M.; Biedermann, D.; Markova, L.; Urbanc, M.; Sarek, J. Pharmacological activities of natural triterpenoids and their therapeutic implications. *Nat. Prod. Rep.* **2006**, *23*, 394–411.
- (2) Kuo-Hsiung, L. Discovery and Development of Natural Product-Derived Chemotherapeutic Agents Based on a Medicinal Chemistry Approach. *J. Nat. Prod.* **2010**, *73*, 500–516.
- (3) Macías, F. A.; Simonet, A. M.; Esteban, M. D. Potential allelopathic lupane triterpenes from bioactive fractions of *Melilotus messanensis*. *Phytochemistry* **1994**, *36*, 1369–1379.
- (4) Silva, S. R. S.; Silva, G. D. F.; Barbosa, L. C. A.; Duarte, L. P.; King-Díaz, B.; Archundia-Camacho, F.; Lotina-Hennsen, B. Uncoupling and inhibition properties of 3,4-seco-friedelan-3-oic acid isolated from *Maytenus imbricata*. *Pestic. Biochem. Physiol.* **2007**, *87*, 109–114.
- (5) Torres-Romero, D.; King-Díaz, B.; Jiménez, I. A.; Lotina-Hennsen, B.; Bazzocchi, I. L. Sesquiterpenes from *Celastrus vulcanicola* as Photosynthetic inhibitors. *J. Nat. Prod.* **2008**, *71*, 1331–1335.
- (6) Bruun, T.; Jefferies, P. R. Triterpenoids in lichens. I. The Occurrence of Friedelin and epiFriedelinol. *Acta Chem. Scand.* **1954**, *8*, 71–75.
- (7) Betancor, C.; Freire, R.; González, A. G.; Salazar, J. A.; Pascard, C.; Prange, T. Three triterpenes and other terpenoids from *Catha cassinoides*. *Phytochemistry* **1980**, *19*, 1989–1993.
- (8) Ramiah, P. A.; Devi, P. U.; Frolow, F.; Lavie, D. 3-Oxo-friedelan-20a-oic acid from *Gymnosporia emarginata*. *Phytochemistry* **1984**, *23*, 2251–2255.
- (9) Strasser, R. J.; Tsimilli-Michael, M.; Srivastava, A. Analysis of the chlorophyll *a* fluorescence transient. In *Chlorophyll fluorescence: A signature of photosynthesis*; Papageorgiou, G. C., Govindjee, Eds.; Kluwer Academic Publishers: Netherlands, 2004; Chapter 12, pp 321–362.
- (10) Morales-Flores, F.; Aguilar, M. I.; King-Díaz, B.; Santiago-Gómez, J.-R. De; Lotina-Hennsen, B. Natural diterpenes from *Croton ciliatoglanduliferus* as photosystem II and photosystem I inhibitors in spinach chloroplasts. *Photosynth. Res.* **2007**, *91*, 71–88.
- (11) Mills, J. D.; Mitchell, P.; Schurrmann, P. Modulation of coupling ATPase activity in intact chloroplasts. *FEBS Lett.* **1980**, *191*, 144–148.
- (12) Strain, H. H.; Cope, B. T.; Svec, W. A. Analytical procedures for the isolation, identification, estimation and investigation of the chlorophylls. *Methods Enzymol.* **1971**, *23*, 452–266.
- (13) Dilley, R. A. Ion transport ( $\text{H}^+$ ,  $\text{K}^+$ ,  $\text{Mg}^{2+}$  exchange phenomena). *Methods Enzymol.* **1972**, *24*, 68–74.
- (14) Aguilar, M. I.; Romero, M. G.; Chávez, M. I.; King-Díaz, B.; Lotina-Hennsen, B. Biflavonoids isolated from *Selaginella lepidophylla* inhibit photosynthesis in spinach chloroplasts. *J. Agric. Food Chem.* **2008**, *56*, 6994–7000.
- (15) Saha, S.; Ouitrakul, R.; Izawa, S.; Good, N. Electron transport and photophosphorylation in chloroplasts as a function of the electron acceptor. *J. Biol. Chem.* **1971**, *246*, 3204–3209.
- (16) Yruela, I.; Montoya, G.; Alonso, P. J.; Picorel, R. Identification of the pheophytin- $\text{Q}_A$ -Fe domain of the reducing side of the photosystem II as the Cu(II)-inhibitory binding site. *J. Biol. Chem.* **1991**, *266*, 22847–22850.
- (17) Guaiquinta, R. T.; Dilley, R. A. A partial reaction in photosystem II: reduction of silicomolybdate prior to the site of dichlorophenyl-dimethyl-urea inhibition. *Biochim. Biophys. Acta* **1975**, *387*, 288–305.
- (18) Allen, J. F.; Holmes, N. G. Electron transport partial reactions. In *Photosynthesis, energy transduction. A practical approach*; Hipkinns, M. F., Baker, N. R., Eds.; IRL Press: Oxford, U.K., 1986; Chapter 5, pp 103–141.
- (19) Sumner, J. B. Scientific apparatus and laboratory methods. A method for the colorimetric determination of phosphorus. *Science* **1944**, *100*, 413–418.
- (20) Strasser, R. J.; Srivastava, A.; Govindjee Polyphasic chlorophyll *a* fluorescence transients in plants and cyanobacteria. *Photochem. Photobiol.* **1995**, *61*, 32–42.

- (21) Panda, D.; Rao, D. N.; Sharma, S. G.; Strasser, R. J.; Sarkar, R. K. Subemergence effects on rice genotypes during seedling stage: Probing of subemergence driven changes of photosystem II by chlorophyll *a* fluorescence induction O-J-I-P transients. *Photosynthetic* **2006**, *44*, 69–75.
- (22) Huan-Xin, J.; Li-Song, C.; Jin-gui, Z.; Shuang, H.; Ning, T.; Brandon, R. S. Aluminum-induced effects on photosystem II photochemistry in *Citrus* leaves assessed by the chlorophyll *a* fluorescence transient. *Tree Physiol.* **2008**, *28*, 1863–1871.
- (23) González-Ibarra, M.; Farfán, N.; Trejo, C.; Uribe, S.; Lotina-Hennsen, B. Selective herbicide activity of 2,5-di(benzylamine)-*p*-benzoquinone against the monocot weed *Echinochloa crusgalli*. An *in vivo* analysis of photosynthesis and growth. *J. Agric. Food Chem.* **2005**, *53*, 3415–3420.
- (24) Joan Saary, M. Radar plots: a useful way for presenting multivariate health care data. *J. Clin. Epidem.* **2008**, *60*, 311–317.
- (25) Schansker, G.; Tóth, S. Z.; Strasser, R. J. Methylviologen and dibromothymoquinone treatments of pea leaves reveal the role of photosystem I in the Chl *a* fluorescence rise OJIP. *Biochim. Biophys. Acta* **2005**, *1706*, 250–261.
- (26) González-Vázquez, R.; King-Díaz, B.; Aguilar, M. I.; Diego, N.; Lotina-Hennsen, B. Pachypodol from *Croton ciliatoglanduliferus* Ort. as water-splitting enzyme inhibitor on thylakoids. *J. Agric. Food Chem.* **2006**, *54*, 1217–1221.
- (27) Morales-Flores, F.; Aguilar, M. I.; King-Díaz, B.; de Santiago-Gómez, J. R.; Lotina-Hennsen, B. Natural diterpenes from *Croton ciliatoglanduliferus* as photosystem II and photosystem I inhibitors in spinach chloroplasts. *Photosynth. Res.* **2007**, *91*, 71–80.
- (28) González-Bernardo, E.; Aguilar, M. I.; Delgado, G.; King-Díaz, B.; Lotina-Hennsen, B. Photosynthetic electron transport interaction of xanthorrhizol isolated from *Iostephane heterophylla* and its derivatives. *Physiol. Plant.* **2003**, *119*, 598–604.
- (29) Bussotti, F.; Strasser, R. J.; Schaub, M. Photosynthetic behavior of woody species under high ozone exposure probed with the JIP-test: A review. *Environ. Pollut.* **2007**, *147*, 430–437.

---

Received for review June 9, 2010. Revised manuscript received September 1, 2010. Accepted September 3, 2010. This work was supported by the Agencia Canaria de Investigación, Innovación y Sociedad de la Información (C200801000049), and PCI-Iberoamérica (A/023081/09, AEI) projects, and the photosynthetic study was financed by Grant IN 211309 from DGAPA, UNAM. D.T.-R. thanks the Gobierno Autónomo de Canarias for the fellowship “Antonio González” and the Servicio de Parques Nacionales y Vida Silvestre, Dirección de Recursos Renovables del Ministerio de Agricultura y Ganadería (MAG) and Fundación Ecológica de El Salvador (SALVANATURA) for supplying the plant material.